Synthesis of Mixed-metal Clusters by the Reaction of the Unsaturated Cluster $[Os_3(\mu\text{-}H)_2(CO)_{10}]$ with Transition-metal Hydrides: the *X*-Ray Crystal Structures of $[Os_3H_3(CO)_{10}\{Cu(PPh_3)\}]$ and $[Os_3H_3(CO)_{11}\{Ir(PPh_3)\}]$ †

Brian F. G. Johnson, Jack Lewis,* Paul R. Raithby, S. N. Azman, B. Syed-Mustaffa, Michael J. Taylor, and Kenton H. Whitmire
University Chemical Laboratory, Lensfield Road, Cambridge CB2 1EW
William Clegg
Anorganisch-Chemisches Institut der Universität, Tammannstrasse 4, D-3400 Göttingen, Federal Republic of Germany

The co-ordinatively unsaturated dihydride cluster $[Os_3(\mu\text{-}H)_2(CO)_{10}]$ reacts with the transition-metal hydrides $[\{CuH(PPh_3)\}_6]$, $[IrH(CO)_2(PPh_3)_2]$, $[RhH(CO)(PPh_3)_2]$, and $[NiH(Cl)(\{P(C_6H_{11})_3\}_2]$ to give the mixed-metal clusters $[Os_3H_3(CO)_{10}\{Cu(PPh_3)\}]$ (1), $[Os_3H_3(CO)_{11}\{Ir(PPh_3)\}]$ (2), $[Os_3H_3(CO)_{11}\{Rh(PPh_3)\}]$ (3), and $[Os_3H_2(CO)_{10}\{Ni[P(C_6H_{11})_3]\}]$ (4). These complexes have been characterized by i.r. and n.m.r. spectroscopy, and the structures of (1) and (2) have been established by single-crystal *X*-ray analysis. In complex (1) the three Os atoms lie at the vertices of an isosceles triangle the long edge [3.026(3) Å] of which is bridged by the Cu atom of the $Cu(PPh_3)$ ligand. The hydrides were not located directly but evidence suggests that they bridge the long Os–Os bond and the two Os–Cu bonds. The carbonyl arrangement is similar to that observed in $[Os_3H_2(CO)_{10}]$. In complex (2) the Ir atom caps the Os_3 triangle to form a distorted tetrahedral metal framework. The three Ir–Os bond lengths [2.759(3), 2.789(2), and 2.917(3) Å] show considerable variation. The distribution of the eleven terminal carbonyl ligands and the phosphine group, which is co-ordinated to the Ir atom, indicates that the three hydrides bridge the two longer Os–Os bonds, and the longest Os–Ir bond. From the spectroscopic data the overall geometry of complex (3) is closely related to that of (2), while (4) has a tetrahedral metal arrangement with hydrides and carbonyl groups bridging Os–Os and Os–Ni edges.

Mixed-metal clusters should exhibit greater reactivity than the analogous homometal complexes since they contain inherent polarity in the mixed-metal bonds. In view of this and because of the catalytic activity of some of these species [1] a considerable research effort has been concentrated on the synthesis and chemistry of these complexes. A wide variety of synthetic routes has been employed in the preparation of mixed-metal carbonyl clusters and their derivatives.[2,3] One very useful starting material in these syntheses has proved to be the unsaturated, 46-electron cluster $[Os_3H_2(CO)_{10}]$,[4] which readily reacts with nucleophiles under relatively mild conditions. This dihydride reacts with many low-valent metal complexes, such as $[Pt(C_2H_4)_2\{P(C_6H_{11})_3\}]$,[5–7] $[Pt(C_2H_4)(PPh_3)_2]$,[5–7] $[Rh(C_2H_4)(acac)]$ (acac = acetylacetonate),[8] $[Ni(C_2H_4)(PPh_3)_2]$,[8] and $[Co_4(CO)_{12}]$,[9] to produce mixed-metal species. In the ethylenic complexes the ethylene group is readily lost which leaves a reactive metal-containing fragment to attack the triosmium cluster.

Hitherto, we have concentrated our attentions on the synthesis and reactivity of mixed osmium–gold clusters using the reactive anion $[Os_3H(CO)_{11}]^-$ or $[Os_3H_2(CO)_{10}]$ in reactions with $[AuCl(PPh_3)]$.[10–13] In this gold complex the Cl atom is displaced and the *sp*-hybridized orbital of the gold(I) atom of the $Au(PPh_3)$ donates one electron to the cluster. In this paper we extend this method of synthesis by the reaction of $[Os_3H_2(CO)_{10}]$ with low-valent transition-metal hydride complexes, which will eliminate stable small molecules such as CO or HCl under reaction conditions, to produce reactive intermediates which add to the trinuclear osmium cluster.

Results and Discussion

When a solution of $[\{CuH(PPh_3)\}_6]$ in tetrahydrofuran (thf) is stirred with $[Os_3H_2(CO)_{10}]$ for *ca.* 40 min the purple colour of the dihydride slowly disappears and is replaced by a greenish yellow colouration. The residual solid was purified by thin-layer chromatography (t.l.c.) and the product (1) isolated as yellow crystals. Examination of the i.r. spectrum of (1) in the carbonyl-stretching region shows ten bands all of which may be assigned to terminal groups (Table 1). The spectrum shows significant differences from that of $[Os_3H(CO)_{10}\{Au(PPh_3)\}]$,[10] prepared by the reaction of $[Os_3H(CO)_{11}]^-$ with $[AuCl(PPh_3)]$, which might be expected to have a related structure to that of (1).

The ^1H n.m.r. spectrum of compound (1) exhibits a resonance that may be assigned to the phenyl rings at δ 7.46 p.p.m., and two resonances in the hydride region at δ −11.8 and −20.47 p.p.m. in a 2 : 1 intensity ratio (Table 1). The latter signal is in the same region as that for the hydride bridging an Os–Os bond in $[Os_3H(CO)_{10}\{Au(PPh_3)\}]$.[10] The other hydride signal, which represents two hydrogens, is probably associated with atoms co-ordinated to the Cu atom. Both hydride signals exhibit coupling with the ^{31}P nucleus and the system remains fluxional down to the solvent limit (*ca.* −100 °C). The ^{13}C-{^1H} decoupled n.m.r. spectrum of (1) at room temperature suggests that the carbonyl groups are fluxional. At −35 °C, however, the ^{13}C-decoupled spectrum exhibits resonances due to the carbonyl and the phosphine

† 2,2,2,3,3,3-Hexacarbonyl-1,2;1,3;2,3-tri-μ-hydrido-2,3-μ-tetracarbonylosmio-1-triphenylphosphinecopperdiosmium(2 *Cu–Os*, 3 *Os–Os*) and 1,1,2,2,2,3,3,3,4,4,4-undecacarbonyl-1,2 : 2,3 : 3,4-tri-μ-hydrido-1-triphenylphosphineiridiumtriosmium (3 *Ir–Os*, 3 *Os–Os*).

Supplementary data available (No. SUP 23997, 40 pp.): thermal parameters, H-atom co-ordinates, least-squares planes, structure factors. See Instructions for Authors, *J. Chem. Soc., Dalton Trans.*, 1984, Issue 1, pp. xvii—xix.

Table 1. Spectroscopic properties of the complexes (1)—(4)

Complex	I.r.,[b] ν_{CO}/cm^{-1}	^1H N.m.r., δ/p.p.m.
(1)[a]	2 098m, 2 075w, 2 060s, 2 048s, 2 043s, 2 022s, 2 009m (sh), 2 002s, 1 991s, 1 971m	7.46 (s, C_6H_5), −11.80 (s, br, Cu–H), −20.47 (s, br, Os–H–Os) at 18 °C[c]
(2)	2 094m, 2 072s, 2 052s, 2 043m, 2 032s, 2 012m, 2 005s, 2 002m, 1 992m, 1 984w, 1 971m, 1 960w	7.47 (s, C_6H_5) and −19.46 to −20.02 (s, br, Os–H–Os) at 18 °C[d] −18.30 (s, br, Os–H–Ir) and −20.03 (s, br, Os–H–Os) at −30 °C −18.30 (s, br, Os–H–Ir), −19.91 (s, br, Os–H–Os), and −20.75 (s, br, Os–H–Os) at −50 °C
(3)[e]	2 096m, 2 072s, 2 053s, 2 041s, 2 014s, 2 008s, 1 994w, 1 986w, 1 971w, 1 963w	7.39 (s, C_6H_5) and −18.19 (s, br, Os–H–Os)[c] at 18 °C
(4)	2 094s, 2 064s, 2 059w, 2 038s, 2 019s, 2 007m, 1 998m, 1 980m, 1 969m, 1 865w, 1 798w	4.15, 1.26 (d, PC_6H_{11}) −14.5 (s, w, NiH), and −20.3 (s, w, Os–H–Os)[c] at 18 °C −14.47 (d, NiHP) and −20.23 (s, Os–H–Os) at −50 °C

[a] ^{13}C N.m.r.: δ 183.17 (1 C), 183.04 (1 C), 178.72 (1 C), 178.51 (1 C), 173.49 (2 C), 170.79 (2 C), and 170.07 p.p.m. (2 C) at −35 °C in CD_2Cl_2. [b] n-Hexane solvent. [c] CD_2Cl_2 solvent. [d] $CDCl_3$ solvent. [e] ^{31}P N.m.r.: δ −138 p.p.m. [d, J(RhP) = 107 Hz] in CD_2Cl_2 at 18 °C.

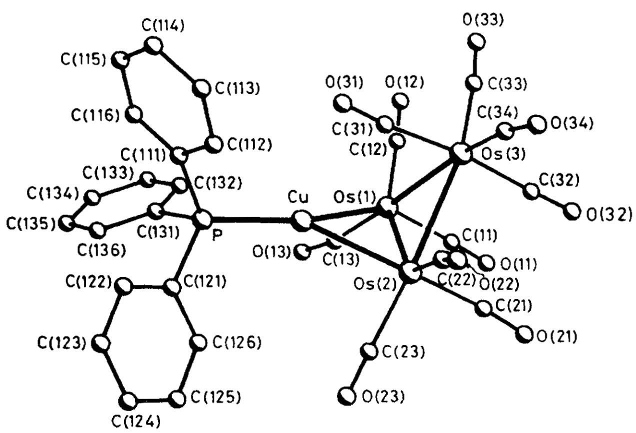

Figure 1. The molecular structure of $[Os_3H_3(CO)_{10}\{Cu(PPh_3)\}]$ (1) including the atom numbering scheme adopted; hydrogen atoms have been omitted for clarity

ligands. In the region of the carbonyl resonances there are seven sets of signals at δ 183.17, 183.04, 178.72, 178.51, 173.49, 170.79, and 170.07 p.p.m. with relative intensities 1 : 1 : 1 : 1 : 2 : 2 : 2, respectively. It is possible to make some tentative assignments of these signals. The set of signals at δ 178.72 and 178.51 p.p.m. correspond to a doublet which is almost certainly caused by the coupling of the carbonyl groups *trans* to the '$Cu(PPh_3)$' fragment with the ^{31}P nucleus, $J(^{13}C^{31}P)$ = 11.5 Hz. The resonances at δ 183.17 and 183.04 p.p.m. with relative intensities of unity may arbitrarily be assigned to the different axial carbonyls of the '$Os(CO)_4$' fragment (Figure 1). The three resonances at δ 173.49, 170.79, and 170.07 p.p.m. of integrated intensity two may then be assigned to the three remaining pairs of carbonyl groups.

The spectroscopic data for (1) are consistent with the formulation $[Os_3H_3(CO)_{10}\{Cu(PPh_3)\}]$, which suggests that the cluster $[\{CuH(PPh_3)\}_6]$ breaks down under mild conditions and a '$CuH(PPh_3)$' unit adds to $[Os_3H_2(CO)_{10}]$. In order to establish the full molecular geometry a single-crystal *X*-ray analysis was undertaken. The structure is shown in Figure 1 while associated bond lengths and interbond angles are listed in Table 2. The arrangement of the non-hydrogen atoms is similar to that observed in the gold analogue, $[Os_3H(CO)_{10}\{Au(PPh_3)\}]$,[10] although the detailed geometry shows some important differences. The three Os atoms lie at the vertices of an isosceles triangle the longer edge of which [Os(1)–Os(2)] is bridged by the Cu atom of the $Cu(PPh_3)$ groups to give a 'butterfly' metal framework. The dihedral angle between the Os(1)Os(2)Os(3) and Os(1)Os(2)Cu planes is 107.8°, which is similar to the value of 109.8° in the gold analogue.[10] Each of the two Os atoms that is bridged by the Cu atom is also bonded to three terminal carbonyl ligands. The third Os atom, Os(3), has four terminal carbonyl ligands bonded to it to give it a distorted octahedral co-ordination geometry. One of these carbonyls, C(31)O(31), is involved in a weak interaction with the Cu atom across the cluster [C(31) ··· Cu 2.97(1) Å]. A similar short contact of 3.22 Å is observed in the gold analogue,[10] and presumably both interactions help to supply electron density to the formally 16-electron metal atom. The hydride ligands were not located directly in the *X*-ray analysis. However, potential-energy calculations based on the techniques developed by Orpen[14] show that one of the hydrides bridges the Os(1)–Os(2) bond, on the opposite side of the Os_3 triangle to the Cu atom; the other two bridge the Os(1)–Cu and Os(2)–Cu bonds, respectively. In view of the differences in metal covalent radii the Cu–H distances are likely to be shorter than the Os–H distances. The proposed positions for these hydrides are consistent with the ^1H n.m.r. data. Rapid hydride exchange around the Os(1)Os(2)Cu triangle occurs at room temperature, as illustrated by the broad signals (Table 1) in a 2 : 1 ratio. The low-temperature spectrum (−95 °C) shows ^1H–^{31}P coupling, the larger J(PH) = 4.45 Hz being associated with the two hydrides directly bonded to the Cu atom, while the smaller J(PH) = 3.50 Hz is associated with the hydride bridging the Os–Os edge. These relatively small couplings suggest that the hydrides remain fluxional at the lower temperature since, on average, each hydride spends two thirds of the time bonded directly to the Cu atom, in which situation a large coupling would be expected, and one third of the time bonded to the two Os atoms, where no coupling would be expected.

In compound (1) the Cu-bridged Os(1)–Os(2) distance is *ca.* 0.33 Å longer than the equivalent Os–Os distance of 2.699(1) Å in the gold analogue.[10] In the latter species the Au atom was considered to be in the 1+ oxidation state. In compound (1) the Cu atom may be considered to be in the 3+ oxidation state, and as such might be expected to adopt the square-planar d^8 configuration with the PPh_3 group and the

Table 2. Bond lengths (Å) and angles (°) for $[Os_3H_3(CO)_{10}\{Cu(PPh_3)\}]$

Os(1)–Os(2)	3.026(3)	P–C(111)	1.819(21)	Os(1)–Os(3)	2.892(3)	Cu–P	2.213(8)
Os(1)–Cu	2.695(5)	P–C(131)	1.823(18)	Os(1)–C(11)	1.942(35)	P–C(121)	1.809(21)
Os(1)–C(12)	1.853(35)	C(12)–O(12)	1.197(43)	Os(1)–C(13)	1.937(29)	C(11)–O(11)	1.125(42)
Os(2)–Os(3)	2.891(3)	C(21)–O(21)	1.158(39)	Os(2)–Cu	2.726(5)	C(13)–O(13)	1.135(36)
Os(2)–C(21)	1.926(33)	C(23)–O(23)	1.099(44)	Os(2)–C(22)	1.886(23)	C(22)–O(22)	1.151(31)
Os(2)–C(23)	1.963(36)	C(32)–O(32)	1.133(37)	Os(3)–C(31)	1.958(34)	C(31)–O(31)	1.102(41)
Os(3)–C(32)	1.987(29)	C(34)–O(34)	1.154(41)	Os(3)–C(33)	1.863(33)	C(33)–O(33)	1.144(43)
Os(3)–C(34)	1.885(32)						

Os(2)–Os(1)–Os(3)	58.4(1)	Cu–P–C(111)	111.4(6)	Os(1)–Os(2)–C(23)	118.8(9)
Os(3)–Os(1)–Cu	85.9(1)	C(111)–P–C(121)	103.6(9)	Cu–Os(2)–C(23)	90.6(10)
Os(3)–Os(1)–C(11)	94.7(9)	C(111)–P–C(131)	104.5(10)	C(22)–Os(2)–C(23)	98.7(12)
Os(2)–Os(1)–C(12)	145.4(8)	Os(1)–C(11)–O(11)	178.2(26)	Os(1)–Os(3)–C(31)	87.6(8)
Cu–Os(1)–C(12)	122.7(9)	Os(1)–C(13)–O(13)	169.1(31)	Os(1)–Os(3)–C(32)	88.5(7)
Os(2)–Os(1)–C(13)	117.0(10)	Os(2)–C(22)–O(22)	168.9(25)	C(31)–Os(3)–C(32)	173.3(14)
Cu–Os(1)–C(13)	86.4(9)	Os(3)–C(31)–O(31)	174.7(32)	Os(2)–Os(3)–C(33)	160.1(8)
C(12)–Os(1)–C(13)	96.7(13)	Os(3)–C(33)–O(33)	174.1(23)	C(32)–Os(3)–C(33)	92.3(13)
Os(1)–Os(2)–Cu	55.6(1)	P–C(111)–C(112)	118.0(6)	Os(2)–Os(3)–C(34)	102.6(13)
Os(1)–Os(2)–C(21)	92.6(10)	P–C(121)–C(122)	123.0(6)	C(32)–Os(3)–C(34)	95.2(14)
Cu–Os(2)–C(21)	144.8(9)	P–C(131)–C(132)	119.0(6)	Os(1)–Cu–Os(2)	67.9(1)
Os(3)–Os(2)–C(22)	83.4(9)	Os(2)–Os(1)–Cu	56.6(1)	Os(2)–Cu–P	141.7(3)
C(21)–Os(2)–C(22)	95.8(12)	Os(2)–Os(1)–C(11)	94.7(10)	Cu–P–C(121)	114.6(7)
Os(3)–Os(2)–C(23)	175.9(10)	Cu–Os(1)–Cu(11)	145.5(11)	Cu–P–C(131)	117.2(6)
C(21)–Os(2)–C(23)	93.2(14)	Os(3)–Os(1)–C(12)	87.2(8)	C(121)–P–C(131)	104.4(9)
Os(1)–Os(3)–Os(2)	63.1(1)	C(11)–Os(1)–C(12)	91.8(15)	Os(1)–C(12)–O(12)	176.5(20)
Os(2)–Os(3)–C(31)	82.6(11)	Os(3)–Os(1)–C(13)	172.3(9)	Os(2)–C(21)–O(21)	174.0(32)
Os(2)–Os(3)–C(32)	90.8(9)	C(11)–Os(1)–C(13)	91.8(13)	Os(2)–C(23)–O(23)	178.5(31)
Os(1)–Os(3)–C(33)	97.3(8)	Os(1)–Os(2)–Os(3)	58.5(1)	Os(3)–C(32)–O(32)	175.2(25)
C(31)–Os(3)–C(33)	93.6(14)	Os(3)–Os(2)–Cu	85.4(1)	Os(3)–C(34)–O(34)	171.2(37)
Os(1)–Os(3)–C(34)	165.4(13)	Os(3)–Os(2)–C(21)	90.1(11)	P–C(111)–C(116)	121.7(7)
C(31)–Os(3)–C(34)	87.3(14)	Os(1)–Os(2)–C(22)	141.0(9)	P–C(121)–C(126)	117.0(6)
C(33)–Os(3)–C(34)	96.7(15)	Cu–Os(2)–C(22)	118.2(9)	P–C(131)–C(136)	121.0(6)
Os(1)–Cu–P	148.3(2)				

two hydrides occupying three of the four sites. A continuation of the P→Cu vector bisects the Os(1)–Os(2) vector so that the fourth lobe of the square-planar hybridized orbital may be thought of as interacting with the Os_2 unit to give a delocalized Os_2Cu bonding system. The Cu–P(1) distance in (1) lies at the shorter end of the range of Cu–P distances [2.217(7)—2.262(7) Å] found in $[\{CuH(PPh_3)\}_6]$ [15] where the Cu atoms are formally five-co-ordinate. The Cu atom bridges the Os(1)–Os(2) bond slightly asymmetrically, but the average Os–Cu distance of 2.711(8) Å is longer than the range of distances [2.527(7)—2.688(8) Å] for the capping Cu atom in the $[Os_{10}C(CO)_{24}\{Cu(NCMe)\}]^-$ anion.[16]

The two unbridged Os–Os bond lengths are equivalent [average 2.892(2) Å], and this distance is only *ca.* 0.01 Å longer than the average Os–Os bond length of 2.877(3) Å in $[Os_3(CO)_{12}]$.[17] However, these bond lengths in the two compounds are significantly longer than the related unbridged distances in $[Os_3H(CO)_{10}\{Au(PPh_3)\}]$ [2.834(3) Å] [10] and $[Os_3(CO)_{10}\{Au(PEt_3)\}_2]$ [2.830(1) Å].[18]

The angles within the Os_3Cu unit in compound (1) show some variations from those found in the Os_3Au unit in $[Os_3H(CO)_{10}\{Au(PPh_3)\}]$,[10] consistent with the variations in metal–metal bond lengths between the two structures. For example, the Os(1)–Cu–Os(2) angle is *ca.* 9° wider than the comparable Os–Au–Os angle of 58.7(1)° in the gold analogue.

The ten carbonyl ligands in compound (1) are all essentially linear, with a maximum deviation of 4σ from the idealized angle. The Os–C(carbonyl) distances may be divided into a number of groups. The longest Os–C bond lengths [average 1.97(2) Å] are associated with the two *trans* axial carbonyls on Os(3). This is consistent with the two *trans* carbonyls, which are good π acceptors, competing for back donation from the same metal orbital, resulting in two relatively weak, long bonds. For the carbonyl groups bonded to Os(1) and Os(2), the Os–C distances for those ligands pseudo-*trans* to Cu [average 1.93(2) Å] are similar in length to those where the carbonyls are *trans* to Os(3) [average 1.95(2) Å]. In contrast, the equatorial carbonyls bonded to Os(3), *trans* to the same metal–metal bonds, are somewhat shorter [average 1.87(2) Å]. This average distance is similar to the mean value of 1.87(2) Å for the Os–C bonds which are effectively *trans* to the hydride bridging the Os(1)–Os(2) bond. In this case the hydride cannot accept back donation of electron density from the metal atoms, and the carbonyls receive the back-donated electron density, effectively shortening the Os–C bonds. The average carbonyl C–O distance is 1.14(2) Å.

When equimolar quantities of $[Os_3H_2(CO)_{10}]$ and $[IrH(CO)_2(PPh_3)_2]$, in dichloromethane, are refluxed for 0.5 h the purple colour of the dihydride changes to the orange of the product (2). This product was separated by t.l.c., and obtained as bright orange crystals from n-hexane. The i.r. spectrum (Table 1) exhibits twelve bands in the terminal carbonyl region.

The ^1H n.m.r. spectrum of compound (2) shows a resonance that may be assigned to the phenyl groups at δ 7.47 p.p.m., and a single broad resonance centred at δ −19.74 p.p.m. which may be assigned to the bridging hydrides. This signal is significantly broader than that observed for the related complex $[Os_3CoH_3(CO)_{12}]$[9] where the three hydrides bridge the three Os–Os bonds. This suggests that the hydride arrangement is somewhat different, and may indicate that at least one hydride bridges an Os–Ir bond. At −30 °C the hydride region of the ^1H n.m.r. spectrum shows two broad signals, at δ −18.30 and −20.03 p.p.m. with relative intensities of 1 : 2 respectively. These two resonances may then be assigned to the hydrides which bridge an Os–Ir and two

Table 3. Bond lengths (Å) and angles (°) for $[Os_3H_3(CO)_{11}\{Ir(PPh_3)\}]$

Os(1)–Ir	2.759(3)	C(32)–Os(3)	1.885(39)	Os(2)–Ir	2.789(2)	C(33)–Os(3)	1.876(41)
Os(3)–Ir	2.917(3)	O(01)–C(01)	1.089(37)	Os(2)–Os(1)	2.925(3)	O(02)–C(02)	1.100(28)
Os(3)–Os(1)	2.787(3)	O(11)–C(11)	1.106(41)	Os(3)–Os(2)	2.934(3)	O(12)–C(12)	1.101(39)
P–Ir	2.366(8)	O(13)–C(13)	1.108(39)	C(01)–Ir	1.921(28)	O(21)–C(21)	1.110(39)
C(02)–Ir	1.909(20)	O(22)–C(22)	1.131(41)	C(11)–Os(1)	1.881(31)	O(23)–C(23)	1.099(36)
C(12)–Os(1)	1.924(28)	O(31)–C(31)	1.115(54)	C(13)–Os(1)	1.933(32)	O(32)–C(32)	1.176(48)
C(21)–Os(2)	1.906(30)	O(33)–C(33)	1.151(55)	C(22)–Os(2)	1.891(31)	C(1P1)–P	1.835(18)
C(23)–Os(2)	1.925(26)	C(2P1)–P	1.828(18)	C(31)–Os(3)	1.911(41)	C(3P1)–P	1.389(20)

Os(2)–Ir–Os(1)	63,5(1)	C(23)–Os(2)–Os(1)	150.6(8)	O(01)–C(01)–Ir	174.9(28)
Os(3)–Ir–Os(2)	61.7(1)	C(31)–Os(3)–Os(1)	167.9(11)	O(11)–C(11)–Os(1)	174.9(31)
Os(3)–Os(1)–Ir	63.5(1)	C(32)–Os(3)–Os(1)	90.7(13)	O(13)–C(13)–Os(1)	178.3(31)
Os(3)–Os(2)–Ir	61.1(1)	C(33)–Os(3)–Os(1)	94.5(14)	O(22)–C(22)–Os(2)	178.6(32)
Os(2)–Os(3)–Ir	57.1(1)	C(11)–Os(1)–Ir	96.0(10)	O(31)–C(31)–Os(3)	176.7(34)
Os(3)–Os(2)–Os(1)	56.8(1)	C(13)–Os(1)–Ir	157.6(10)	O(33)–C(33)–Os(3)	173.7(40)
P–Ir–Os(1)	168.4(2)	C(22)–Os(2)–Ir	164.3(10)	C(01)–Ir–Os(2)	156.9(8)
P–Ir–Os(3)	112.4(2)	C(31)–Os(3)–Ir	114.4(11)	C(02)–Ir–Os(1)	87.3(8)
C(2P1)–P–Ir	113.9(7)	C(33)–Os(3)–Ir	100.6(12)	C(02)–Ir–Os(3)	142.6(7)
C(2P1)–P–C(1P1)	98.5(9)	C(12)–Os(1)–C(11)	93.4(13)	C(11)–Os(1)–Os(3)	97.3(10)
C(3P1)–P–C(2P1)	101.5(9)	C(13)–Os(1)–C(12)	97.9(13)	C(12)–Os(1)–Os(3)	163.2(9)
C(1P6)–C(1P1)–P	120.7(13)	C(23)–Os(2)–C(21)	92·5(13)	C(13)–Os(1)–Os(3)	94.8(10)
C(2P6)–C(2P1)–P	117.8(14)	C(32)–Os(3)–C(31)	94.8(17)	C(21)–Os(2)–Os(3)	154.4(9)
C(3P6)–C(3P1)–P	116.9(15)	C(33)–Os(3)–C(32)	90.5(17)	C(22)–Os(2)–Os(3)	105.5(9)
C(02)–Ir–P	98.8(8)	Os(3)–Ir–Os(1)	58.7(1)	C(23)–Os(2)–Os(3)	101.7(9)
O(02)–C(O2)–Ir	177.5(24)	Os(2)–Os(1)–Ir	58.9(1)	C(31)–Os(3)–Os(2)	106.8(11)
O(12)–C(12)–Os(1)	172,3(26)	Os(1)–Os(2)–Ir	57.6(1)	C(32)–Os(3)–Os(2)	101.2(11)
O(21)–C(21)–Os(2)	172.1(27)	Os(1)–Os(3)–Ir	57.8(1)	C(33)–Os(3)–Os(2)	152.9(13)
O(23)–C(23)–Os(2)	178.6(23)	Os(3)–Os(1)–Os(2)	61.8(1)	C(12)–Os(1)–Ir	102.5(8)
C(32)–C(32)–Os(3)	171.3(33)	Os(2)–Os(3)–Os(1)	61.4(1)	C(21)–Os(2)–Ir	96.7(8)
C(01)–Ir–Os(1)	94.2(9)	P–Ir–Os(2)	106.4(2)	C(23)–Os(2)–Ir	95.5(7)
C(01)–Ir–Os(3)	102.7(8)	C(1P1)–P–Ir	120.7(6)	C(32)–Os(3)–Ir	147.0(13)
C(02)–Ir–Os(2)	90.6(7)	C(3P1)–P–Ir	114.3(7)	C(02)–Ir–C(01)	94.2(11)
C(11)–Os(1)–Os(2)	152.0(10)	C(3P1)–P–C(1P1)	105.3(9)	C(13)–Os(1)–C(11)	91.8(13)
C(12)–Os(1)–Os(2)	103.6(9)	C(1P2)–C(1P1)–P	119.3(12)	C(22)–Os(2)–C(21)	94.2(12)
C(13)–Os(1)–Os(2)	107.4(10)	C(2P2)–C(2P1)–P	121.5(14)	C(23)–Os(2)–C(22)	95.3(13)
C(21)–Os(2)–Os(1)	101.6(9)	C(3P2)–C(3P1)–P	123.0(12)	C(33)–Os(3)–C(31)	96.2(18)
C(22)–Os(2)–Os(1)	109.0(11)	C(01)–Ir–P	95.2(9)		

Os–Os bonds, respectively. A further reduction in the temperature at which the spectrum is run, to −50 °C, results in a further splitting of the signal at δ −20.03 p.p.m. to produce two resonances at δ −19.91 and −20.75 p.p.m. This suggests that the two hydrides which bridge the Os–Os bonds are not equivalent.

In order to confirm these spectroscopic assignments and to establish the overall molecular geometry a single-crystal *X*-ray analysis was undertaken. The molecular structure of $[Os_3H_3(CO)_{11}\{Ir(PPh_3)\}]$ (2) is illustrated in Figure 2 and the associated bond lengths and angles are presented in Table 3. The four metal atoms lie at the vertices of a distorted tetrahedron, a common metal-atom framework geometry in heteronuclear metal clusters.[19] The three Os atoms define a near isosceles triangle which is asymmetrically capped by the Ir atom. This metal atom is also co-ordinated to the terminal triphenylphosphine ligand and two terminal carbonyl groups. Each of the three Os atoms is co-ordinated to three terminal carbonyl ligands. The three bridging hydride ligands were not located directly in the *X*-ray analysis, but from the distribution of the carbonyl groups, coupled with the lengths of the metal–metal bonds, it appears that they bridge the two Os–Os bonds Os(1)–Os(2) and Os(2)–Os(3), and the Os(3)–Ir bond. The metal–metal–C(carbonyl) angles *cis* to these edges average 108(1)°, compared to an average of 95(2)° for the other three edges, which suggests that the steric requirements of the hydrides may cause the carbonyls to bend back. Churchill and Hollander [20] have made a careful study of the hydride positions in the tetranuclear complex $[Os_3W(\mu\text{-}H)_3(CO)_{11}(\eta^5\text{-}C_5H_5)]$ and have shown that similar trends are observed for the hydride-bridged bonds.

The two long Os–Os bonds [Os(1)–Os(2) and Os(2)–Os(3), average 2.930(2) Å], which are hydride bridged, are slightly shorter than the average value of 2.964(2) Å for the hydride-bridged Os–Os bonds in $[Os_4(\mu\text{-}H)_4(CO)_{12}]$.[21] These two bonds are also somewhat shorter than the hydride-bridged Os–Os bond in the tetrahedral cluster $[Os_3Ir(\mu\text{-}H)_2(\mu\text{-}Cl)(\mu\text{-}CO)(CO)_9(PPh_3)]$ [22] [3.005(1) Å], or in the 'butterfly' cluster $[Os_3Ir(\mu\text{-}H)_2(\mu\text{-}Cl)(CO)_{12}]$ [23] [2.994(1) Å]. The third, unbridged Os(1)–Os(3) bond is *ca.* 0.16 Å shorter than the bridged bonds in compound (2), and slightly shorter than the average value of 2.817(2) Å for the unbridged Os–Os bonds in $[Os_4(\mu\text{-}H)_4(CO)_{12}]$.[21] The two unbridged Os–Ir bonds in (2) [average 2.779(4) Å] are similar to the average unbridged distance of 2.776(5) Å in the 'butterfly' cluster $[Os_3Ir(\mu\text{-}H)_2(\mu\text{-}Cl)(CO)_{12}]$,[23] but shorter than the comparative distance of 2.881(1) Å in the tetrahedral cluster $[Os_3Ir(\mu\text{-}H)_2(\mu\text{-}Cl)(\mu\text{-}CO)_9(PPh_3)]$.[22] The bridged Os(3)–Ir bond, in contrast, is slightly longer than the hydride-bridged bond in $[Os_3Ir(\mu\text{-}H)_2(\mu\text{-}Cl)(CO)_{12}]$ [23] [2.096(1) Å].

The Ir–P distance in compound (2) is *ca.* 0.05 Å longer than the average value of 2.312(5) Å for the Ir–P distance in the methylphosphine complex $[Ir_4(CO)_8(PMe_3)_4]$.[24] This Ir–P bond length in the mixed-metal cluster (2) is also significantly longer than equivalent bonds in a number of other iridium clusters.[25]

The high estimated standard deviations on the carbonyl positions make it impossible to assess the bonding in these

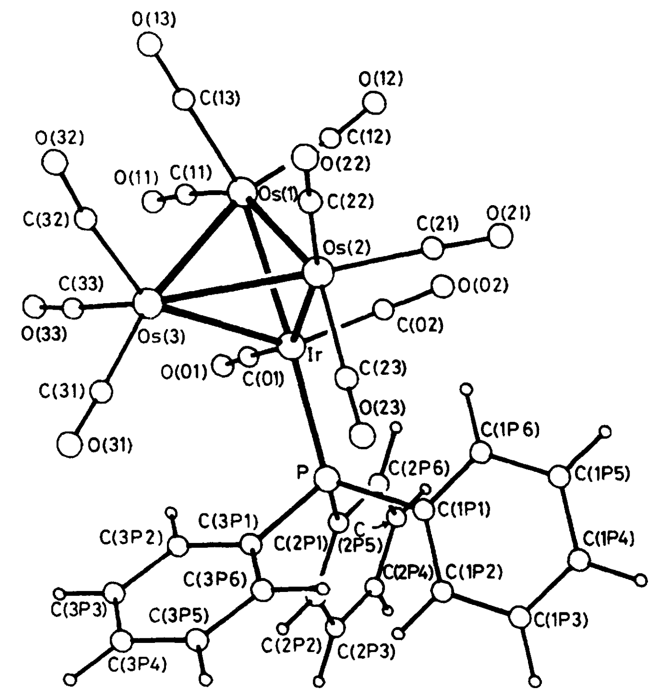

Figure 2. The molecular structure of $[Os_3H_3(CO)_{11}\{Ir(PPh_3)\}]$ (2) including the atom numbering scheme adopted

groups. The average Ir–C(carbonyl) bond length is 1.92(3) Å and the average C–O bond length is 1.10(3) Å for these ligands. The corresponding average Os–C and C–O bond lengths are 1.90(4) and 1.12(4) Å, respectively.

Addition of a dichloromethane solution of $[RhH(CO)(PPh_3)_3]$ to $[Os_3(\mu\text{-}H)_2(CO)_{10}]$ in the same solvent at room temperature resulted in a slow change (2 h) of colour from purple to orange-yellow. Chromatography of the mixture afforded the orange crystalline compound $[Os_3H_3(CO)_{11}\{Rh(PPh_3)\}]$ (3), characterized by microanalysis, and by its i.r., ^1H, and ^{31}P n.m.r. spectra.

The i.r. spectrum of compound (3) exhibits ten signals in the region normally assigned to terminal carbonyl groups. The ^1H n.m.r. spectrum shows a broad high-field signal at δ −18.19 p.p.m., as well as a resonance due to the triphenylphosphine ligand. In the room-temperature spectrum this broad signal did not show coupling with the ^{31}P nucleus; as in the room-temperature ^1H n.m.r. spectrum of $[Os_3H_3(CO)_{11}\{Ir(PPh_3)\}]$ (2), the absence of an observable coupling may be attributed to the broadness of the signal. The ^{31}P n.m.r. spectrum shows one doublet at δ −138 p.p.m. which exhibits coupling to the ^{103}Rh nucleus [J(RhP) 107 Hz]. In view of the similarity between the spectra of $[Os_3H_3(CO)_{11}\{Ir(PPh_3)\}]$ (2) and $[Os_3H_3(CO)_{11}\{Rh(PPh_3)\}]$ (3) it is probable that the structures are similar. The broadness of the hydride signal of (3) suggests that the distribution of the hydrides probably includes at least one spanning an Os–Rh bond, and unlike the distribution of the hydrides in the related Os_3Co cluster $[Os_3CoH_3(CO)_{12}]$,[9] where the three Os–Os edges are bridged. Both the rhodium and iridium complexes are 'electron-precise' 60-electron species, and neither readily undergoes addition reactions with carbon monoxide or phosphines.

Addition of a dichloromethane solution of $[NiH(Cl)\{P(C_6H_{11})_3\}_2]$ to $[Os_3(\mu\text{-}H)_2(CO)_{10}]$ in the same solvent followed by heating under reflux for 0.5 h led to the disappearance of the initial purple colour and the formation of the orange-red product. This product was purified by chromatography and characterized by i.r. and ^1H n.m.r. spectroscopy as $[Os_3H_2(CO)_{10}\{Ni[P(C_6H_{11})_3]\}]$ (4).

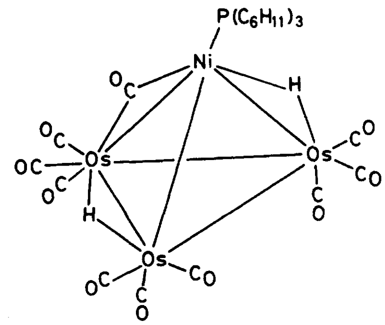

Figure 3. Proposed structure of $[Os_3H_2(CO)_{10}\{Ni[P(C_6H_{11})_3]\}]$ (4)

The i.r. spectrum of compound (4) in the carbonyl-stretching region shows nine bands which may be assigned to terminal carbonyl groups and two bands which may be assigned to edge-bridging groups (Table 1). The presence of bridging carbonyl groups in this complex is in contrast to the situation in the platinum analogue $[Os_3H_2(CO)_{10}\{Pt[P(C_6H_{11})_3]\}]$,[5] and the i.r. spectrum shows similarities to the related complex $[Os_3H_2(\mu\text{-}CO)_2(CO)_8\{Ni(PPh_3)_2\}]$ [8] where two carbonyl groups bridge Os–Ni bonds.

The ^1H n.m.r. spectrum, at room temperature, shows two signals due to the $P(C_6H_{11})_3$ group, and two high-field signals at δ −14.5 and −20.3 p.p.m. However, at −50 °C the lower of these two hydride signals splits into a doublet centred at δ −14.5 p.p.m., J(PH) = 14.6 Hz. This splitting is caused by ^{31}P coupling, and may be assigned to an Os(μ-H)Ni system. The other signal at δ −20.3 p.p.m. did not show splitting at the lower temperature, and may be assigned to a hydride bridging an Os–Os bond. The absence of splitting for this signal sugests that there are no phosphines co-ordinated to the hydride-bridged Os atoms.

The spectroscopic data for (4) are consistent with a structure resembling that of $[Os_3H_2(CO)_{10}\{Pt[P(C_6H_{11})_3]\}]$,[5] where an *X*-ray analysis shows that the Pt caps an Os_3 triangle to form a tetrahedral metal framework. Each Os atom is bonded to three terminal carbonyl ligands while the Pt atom is bonded to one terminal carbonyl and the phosphine ligand. One hydride is considered to bridge an Os–Pt edge and the other an Os–Os edge. In compound (4) it is probable that the overall geometry is related except that at least the carbonyl group associated with the Ni atom becomes involved in bridge bonding (Figure 3). This complex is formally an unsaturated 58-electron species having one electron pair less than that required for a *closo*-tetrahedral cluster. The proposed tetrahedral geometry may be explained, however, if the Ni atom does not adopt the rare-gas configuration but forms stable 16-electron complexes.

Experimental

The complex $[Os_3H_2(CO)_{10}]$ and the transition-metal hydrido-complexes were prepared by literature methods.[26–29] Schlenk-tube techniques were used throughout the experiments and all reactions were performed under a N_2 atmosphere. Reaction solvents were purified, dried, and deoxygenated by distillation under N_2 over appropriate drying agents. The solvents were stored under N_2.

Product separation was achieved using thin-layer chromatography (t.l.c.) with plates precoated to 0.25 mm thickness with Merck Kieselgel $60F_{254}$.

Table 4. Atom co-ordinates ($\times 10^4$) for $[Os_3H_3(CO)_{10}\{Cu(PPh_3)\}]$

Atom	*X*/*a*	*Y*/*b*	*Z*/*c*	Atom	*X*/*a*	*Y*/*b*	*Z*/*c*
Os(1)	5 874(1)	3 047(1)	−1 120(1)	C(122)	8 553(15)	−1 637(13)	−1 240(9)
Os(2)	8 155(1)	2 962(1)	−1 298(1)	C(123)	9 126(15)	−2 034(13)	−1 714(9)
Os(3)	7 679(1)	3 908(1)	−30(1)	C(124)	9 016(15)	−1 623(13)	−2 416(9)
Cu	7 067(3)	1 382(3)	−945(2)	C(125)	8 335(15)	−814(13)	−2 643(9)
P	7 121(5)	−251(6)	−884(5)	C(126)	7 762(15)	−417(13)	−2 169(9)
C(11)	5 496(25)	4 257(26)	−1 688(20)	C(131)	5 828(14)	−901(11)	−1 106(12)
C(12)	5 021(23)	3 387(23)	−494(18)	C(132)	4 908(14)	−407(11)	−1 029(12)
C(13)	4 776(23)	2 308(24)	−1 829(18)	C(133)	3 913(14)	−892(11)	−1 189(12)
C(21)	8 002(23)	4 210(24)	−1 810(19)	C(134)	3 837(14)	−1 873(11)	−1 428(12)
C(22)	9 604(20)	3 157(20)	−753(16)	C(135)	4 757(14)	−2 367(11)	−1 505(12)
C(23)	8 418(24)	2 238(24)	−2 146(19)	C(136)	5 753(14)	−1 882(11)	−1 345(12)
C(31)	7 984(24)	2 588(25)	403(19)	O(11)	5 278(20)	4 945(16)	−2 033(15)
C(32)	7 377(21)	5 176(22)	−582(17)	O(12)	4 433(17)	3 568(17)	−107(13)
C(33)	6 917(21)	4 299(22)	647(17)	O(13)	4 074(16)	1 837(19)	−2 150(13)
C(34)	9 062(28)	4 281(28)	548(21)	O(21)	7 954(22)	4 922(14)	−2 161(14)
C(111)	7 812(15)	−674(14)	45(12)	O(22)	10 527(17)	3 171(16)	−502(13)
C(112)	8 796(15)	−232(14)	400(12)	O(23)	8 588(20)	1 840(17)	−2 616(13)
C(113)	9 302(15)	−463(14)	1 138(12)	O(31)	8 154(19)	1 876(17)	696(14)
C(114)	8 824(15)	−1 136(14)	1 522(12)	O(32)	7 272(21)	5 923(15)	−866(16)
C(115)	7 840(15)	−1 578(14)	1 167(12)	O(33)	6 395(20)	4 468(17)	1 045(14)
C(116)	7 334(15)	−1 347(14)	429(12)	O(34)	9 930(20)	4 556(23)	818(16)
C(121)	7 872(15)	−829(15)	−1 468(9)				

Table 5. Atom co-ordinates ($\times 10^4$) for $[Os_3H_3(CO)_{11}\{Ir(PPh_3)\}]$

Atom	*X*/*a*	*Y*/*b*	*X*/*c*	Atom	*X*/*a*	*Y*/*b*	*Z*/*c*
Ir	562(1)	2 903(1)	3 971(1)	C(01)	−1 449(33)	2 425(17)	3 768(13)
Os(1)	945(1)	2 348(1)	5 100(1)	C(02)	−184(29)	3 913(10)	4 245(11)
Os(2)	3 448(1)	3 171(1)	4 641(1)	C(11)	−845(35)	1 695(18)	5 010(14)
Os(3)	2 478(1)	1 469(1)	4 342(1)	C(12)	34(34)	3 222(15)	5 487(13)
P	771(8)	3 325(4)	3 020(3)	C(13)	1 852(36)	1 735(19)	5 778(15)
C(1P1)	1 638(22)	4 324(10)	2 888(7)	C(21)	3 117(32)	4 299(18)	4 824(13)
C(1P2)	1 802(22)	4 541(10)	2 325(7)	C(22)	5 276(38)	3 075(19)	5 184(15)
C(1P3)	2 388(22)	5 315(10)	2 213(7)	C(23)	4 463(32)	3 468(19)	4 001(9)
C(1P4)	2 810(22)	5 873(10)	2 665(7)	C(31)	3 691(42)	1 090(22)	3 787(17)
C(1P5)	2 647(22)	5 657(10)	3 229(7)	C(32)	3 595(45)	878(23)	4 965(19)
C(1P6)	2 060(22)	4 883(10)	3 340(7)	C(33)	1 010(48)	620(25)	4 219(19)
C(2P1)	−1 080(20)	3 462(12)	2 550(8)	O(01)	−2 544(28)	2 115(15)	3 629(13)
C(2P2)	−1 287(20)	3 245(12)	1 966(8)	O(02)	−569(28)	4 508(10)	4 398(11)
C(2P3)	−2 633(20)	3 470(12)	1 600(8)	O(11)	−1 883(32)	1 302(18)	4 918(12)
C(2P4)	−3 773(20)	3 912(12)	1 818(8)	O(12)	−377(33)	3 699(15)	5 761(11)
C(2P5)	−3 567(20)	4 129(12)	2 402(8)	O(13)	2 342(31)	1 388(18)	6 173(9)
C(2P6)	−2 220(20)	3 904(12)	2 768(8)	O(21)	3 091(28)	4 970(15)	4 922(12)
C(3P1)	1 714(20)	2 566(9)	2 609(9)	O(22)	6 385(22)	3 027(19)	5 502(14)
C(3P2)	3 099(20)	2 722(9)	2 412(9)	O(23)	5 069(28)	3 641(18)	3 644(9)
C(3P3)	3 777(20)	2 107(9)	2 119(9)	O(31)	4 380(37)	832(21)	3 469(14)
C(3P4)	3 071(20)	1 337(9)	2 024(9)	O(32)	4 401(37)	602(20)	5 370(13)
C(3P5)	1 686(20)	1 180(9)	2 221(9)	O(33)	24(43)	145(20)	4 168(13)
C(3P6)	1 008(20)	1 795(9)	2 513(9)				

Infrared spectra between 2 150 and 1 600 cm^{-1} were recorded on a Perkin-Elmer 257 spectrometer with the absorption of CO(g) at 2 143 cm^{-1} as calibrant. Nuclear magnetic resonance spectra were recorded on the University of Cambridge C.F.T. 20 and the Bruker 400 spectrometers.

Preparations.—$[Os_3H_3(CO)_{10}\{Cu(PPh_3)\}]$ (1). A solution of $[Os_3H_2(CO)_{10}]$ (75 mg, 0.08 mmol) in tetrahydrofuran (thf) (1 cm^3) was added to a well stirred solution of $[\{CuH(PPh_3)\}_6]$ (51 mg, 0.1 mmol) in the same solvent by means of a transfer tube. The reaction mixture was stirred for 40 min at room temperature, during which time the purple colour of the dihydride disappeared, and the greenish yellow colour of the product appeared. The solvent was removed under vacuum, and the dried residue was dissolved in a minimum of CH_2Cl_2 and loaded onto preparative t.l.c. plates for separation. Using a 1 : 2 ratio of CH_2Cl_2–n-hexane as eluant, $[Os_3H_3(CO)_{10}\{Cu(PPh_3)\}]$ was obtained (47.3 mg, 45%) which recrystallized in n-hexane to give yellow crystals.

$[Os_3H_3(CO)_{11}\{Ir(PPh_3)\}]$ (2). The compounds $[Os_3H_2(CO)_{10}]$ (40 mg, 0.05 mmol) and $[IrH(CO)_2(PPh_3)_2]$ (35 mg, 0.05 mmol) in CH_2Cl_2 (5 cm^3) were refluxed for 0.5 h during which time the purple colour of the dihydride was replaced by the orange colour of the product. The reaction mixture was cooled to room temperature and the volume of the solvent reduced to *ca.* 1 cm^3. The solution was chromatographed on preparative t.l.c. plates using a 1 : 2 ratio of CH_2Cl_2–n-hexane as eluant to give $[Os_3H_3(CO)_{11}\{Ir(PPh_3)\}]$ (30.9 mg, 50%) which crystallized from n-hexane as bright orange crystals (Found: C, 25.9; H, 1.40; P, 2.50. $C_{29}H_{18}IrO_{11}Os_3P$ requires C, 26.1; H, 1.35; P, 2.30%).

$[Os_3H_3(CO)_{11}\{Rh(PPh_3)\}]$ (3). The compounds $[Os_3H_2$-

$(CO)_{10}]$ (60 mg, 0.07 mmol) and $[RhH(CO)(PPh_3)_3]$ (50 mg, 0.05 mmol) in CH_2Cl_2 (5 cm^3) were stirred together at room temperature for 2 h during which time the purple colour of the dihydride was replaced by the orange-yellow colour of the product. The volume of the solvent was reduced under vacuum to *ca.* 1 cm^3, and the reaction mixture was chromatographed on preparative t.l.c. plates using a 1 : 2 ratio of CH_2Cl_2–n-hexane as eluant to give $[Os_3H_3(CO)_{11}\{Rh(PPh_3)\}]$ (38.2 mg, 43%) which recrystallized from n-hexane as orange crystals (Found: C, 27.6; H, 1.45; P, 2.50. $C_{29}H_{18}O_{11}Os_3PRh$ requires C, 27.9; H, 1.45; P, 2.50%).

$[Os_3H_2(CO)_{10}\{Ni[P(C_6H_{11})_3]\}]$ (4). The compounds $[Os_3H_2(CO)_{10}]$ (18 mg, 0.02 mmol) and $[NiH(Cl)\{P(C_6H_{11})_3\}_2]$ (25 mg, 0.01 mmol) in CH_2Cl_2 (2 cm^3) were refluxed for 0.5 h during which time the purple colour of the dihydride disappeared and was replaced by the orange-yellow colour of the product. Without further reduction of the volume of the reaction mixture, the solution was chromatographed on preparative t.l.c. plates using a 1 : 2 ratio of CH_2Cl_2–n-hexane as eluant to give $[Os_3H_2(CO)_{10}\{Ni[P(C_6H_{11})_3]\}]$ which was recrystallized from n-hexane as orange-red crystals.

Crystal-structure Determination of $[Os_3H_3(CO)_{10}\{Cu(PPh_3)\}]$ (1).—A single crystal with dimensions *ca.* 0.37 × 0.28 × 0.15 mm was mounted on a glass fibre with epoxy-resin, and the space group and approximate cell dimensions determined *via* Weissenberg (Cu) *X*-ray photography.

The crystal was transferred to a Stoe-Siemens four-circle diffractometer, and accurate cell dimensions determined from the angular measurement of 48 reflections in the range $15 < 2\theta < 25°$. 4 536 Profile-fitted intensities [30] were recorded in the range $5.0 < 2\theta < 45.0°$ using graphite-monochromated Mo-K_α radiation and a 24-step ω–θ scan technique. The step width ranged between 0.05 and 0.08°, and the time for each step varied between 0.75 and 3.00 s depending upon the intensity determined in an 18 s initial scan; for reflections giving $I < 6\sigma(I)$ on the prescan, this intensity was retained and no further measurement was made. Three check reflections were monitored periodically throughout the course of data collection but showed no significant variations.

A semiempirical absorption correction based on a pseudo-ellipsoid model and 300 azimuthal scan data from seven independent reflections was applied; transmission factors for the full data set ranged from 0.023 to 0.105. Lorentz polarization corrections were also applied and equivalent reflections averaged to give 2 401 unique observed intensities $[F > 5\sigma(F)]$.

Crystal data. $C_{28}H_{18}CuO_{10}Os_3P$, $M = 1\,179.54$, monoclinic, $a = 12.801(2)$, $b = 13.539(2)$, $c = 18.650(7)$ Å, $\beta = 105.20(2)°$, $U = 3\,119.2$ Å^3, D_m not measured, $Z = 4$, $D_c = 2.51$ g cm^{-3}, $F(000) = 2\,152$, Mo-K_α radiation, $\lambda = 0.710\,69$ Å, $\mu(\text{Mo-}K_\alpha) = 129.42$ cm^{-1}, space group $P2_1/c$ from systematic absences.

The three Os and the Cu atom positions were located by multisolution Σ_2 sign expansion, and all the remaining non-hydrogen atoms from a subsequent electron-density difference synthesis. The structure was refined by blocked-cascade least squares with the Os, Cu, P, and O atoms assigned anisotropic thermal parameters. The carbonyl and phenyl C atoms were assigned individual isotropic thermal parameters, and the phenyl rings were refined as rigid groups with idealized geometry (C–C 1.395 Å, C–C–C 120.0°). The phenyl-hydrogen atoms were placed in idealized positions and constrained to ride on the relevant C atoms (C–H 1.08 Å, C–C–H 120.0°); the H atoms were assigned a common isotropic thermal parameter. In the final cycles of refinement the weighting scheme $w = [\sigma^2(F) + 0.0025|F|^2]^{-1}$ was introduced. The converged residuals were $R = 0.067$ and $R' = \Sigma w^{\frac{1}{2}}\Delta/\Sigma w^{\frac{1}{2}}F_o =$ 0.069. A final electron-density difference synthesis revealed ripples of *ca.* 1.5 e Å^{-3} close to the Os atom positions but did not reveal the positions of the hydride atoms.

Crystal-structure Determination of $[Os_3H_3(CO)_{11}\{Ir(PPh_3)\}]$ (2).—A single crystal with dimensions *ca.* 0.41 × 0.27 × 0.23 mm was mounted on a glass fibre, and the space group and cell dimensions determined as for compound (1).

The crystal was transferred to a Stoe-Siemens diffractometer and data collected using similar techniques and parameters to those employed for (1). A total of 6 435 profile-fitted intensities [30] was recorded. Semiempirical absorption, Lorentz, and polarization corrections were applied, and equivalent reflections averaged to give 3 145 unique observed intensities $[F > 6\sigma(F)]$.

Crystal data. $C_{29}H_{18}IrO_{11}Os_3P$, $M = 1\,258.82$, monoclinic, $a = 8.810(2)$, $b = 16.170(7)$, $c = 23.420(7)$ Å, $\beta = 99.27(1)°$, $U = 3\,292.8$ Å^3, D_m not measured, $Z = 4$, $D_c = 2.54$ g cm^{-3}, $F(000) = 2\,400$, Mo-K_α radiation, $\lambda = 0.710\,69$ Å, $\mu(\text{Mo-}K_\alpha) = 158.95$ cm^{-1}, space group $P2/_1c$ from systematic absences.

The structure was solved using the same techniques as for compound (1). It was refined by blocked full-matrix least squares with the Ir, Os, P, and O atoms assigned anisotropic thermal parameters, and the C atoms individual isotropic thermal parameters. The phenyl rings and their associated H atoms were treated in the same way as for (1). The weighting scheme $w = [\sigma^2(F) + 0.0025|F|^2]^{-1}$ was introduced. The converged residuals were $R = 0.068$ and $R' = \Sigma w^{\frac{1}{2}}\Delta/\Sigma w^{\frac{1}{2}}F_o =$ 0.069. The hydride ligands were not located directly, and a final electron-density difference map revealed ripples of *ca.* 2.4 e Å^{-3} close to the heavy atoms.

The final atomic co-ordinates for complexes (1) and (2) are presented in Tables 4 and 5, respectively. Complex neutral-atom scattering factors [31] were employed in both structure solutions and refinements. All computations were performed on an IBM 370/165 computer at the University of Cambridge using programs written by Professor G. M. Sheldrick.[32] The molecular plots were drawn using the PLUTO program written by Dr. W. D. S. Motherwell.

Acknowledgements

We thank the S.E.R.C. and N.A.T.O. (K. H. W.) for financial support.

References

1 J. S. Bradley, R. L. Pruett, E. Hill, G. B. Ansell, M. E. Leonowicz, and M. A. Modrick, *Organometallics*, 1982, **1**, 748.
2 P. Chini and B. Heaton, *Top. Curr. Chem.*, 1977, **71**, 1.
3 W. L. Gladfelter and G. L. Geoffroy, *Adv. Organomet. Chem.*, 1980, **18**, 207.
4 B. F. G. Johnson, J. Lewis, and P. A. Kilty, *J. Chem. Soc. A*, 1968, 2589.
5 L. J. Farrugia, J. A. K. Howard, P. Mitrprachachon, F. G. A. Stone, and P. Woodward, *J. Chem. Soc., Dalton Trans.*, 1981, 155.
6 L. J. Farrugia, J. A. K. Howard, P. Mitrprachachon, F. G. A. Stone, and P. Woodward, *J. Chem. Soc., Dalton Trans.*, 1981, 162.
7 L. J. Farrugia, J. A. K. Howard, O. Mitrprachachon, F. G. A. Stone, and P. Woodward, *J. Chem. Soc., Dalton Trans.*, 1981, 1274.
8 L. J. Farrugia, J. A. K. Howard, P. Mitrprachachon, F. G. A. Stone, and P. Woodward, *J. Chem. Soc., Dalton Trans.*, 1981, 171.
9 S. Bhaduri, B. F. G. Johnson, J. Lewis, P. R. Raithby, and D. J. Watson, *J. Chem. Soc., Chem. Commun.*, 1978, 343.

10 B. F. G. Johnson, D. A. Kaner, J. Lewis, and P. R. Raithby, *J. Organomet. Chem.*, 1981, **215**, C33.

11 B. F. G. Johnson, D. A. Kaner, J. Lewis, and P. R. Raithby, *J. Chem. Soc., Chem. Commun.*, 1981, 753.

12 B. F. G. Johnson, D. A. Kaner, J. Lewis, P. R. Raithby, and M. J. Taylor, *Polyhedron*, 1982, **1**, 753.

13 B. F. G. Johnson, D. A. Kaner, J. Lewis, P. R. Raithby, and M. J. Taylor, *J. Chem. Soc., Chem. Commun.*, 1982, 314.

14 A. G. Orpen, *J. Chem. Soc., Dalton Trans.*, 1980, 2509.

15 M. R. Churchill, S. A. Bezman, J. A. Osborn, and J. Wormald, *Inorg. Chem.*, 1972, **11**, 1818.

16 B. F. G. Johnson, J. Lewis, W. J. H. Nelson, M. D. Vargas, D. Braga, and M. McPartlin, *J. Organomet. Chem.*, 1983, **246**, C69.

17 M. R. Churchill and B. G. DeBoer, *Inorg. Chem.*, 1977, **16**, 878.

18 K. Burgess, B. F. G. Johnson, D. A. Kaner, J. Lewis, P. R. Raithby, and S. N. A. B. Syed-Mustaffa, *J. Chem. Soc., Chem. Commun.*, 1983, 455.

19 M. Green, D. R. Hankey, M. Murray, A. G. Orpen, and F. G. A. Stone, *J. Chem. Soc., Chem. Commun.*, 1981, 689; S. G. Shore, W-L. Hsu, C. R. Weisenberger, M. L. Caste, M. R. Churchill, and C. Bueno, *Organometallics*, 1983, **1**, 1405; M. Castiglioni, E. Sappa, M. Valle, M. Lanfranchi, and A. Tiripicchio, *J. Organomet. Chem.*, 1983, **241**, 99; L. J. Farrugia, M. Green, D. R. Hankey, A. G. Orpen, and F. G. A. Stone, *J. Chem. Soc., Chem. Commun.*, 1983, 310.

20 M. R. Churchill and F. J. Hollander, *Inorg. Chem.*, 1979, **18**, 161.

21 B. F. G. Johnson, J. Lewis, P. R. Raithby, and C. Zuccaro, *Acta Crystallogr., Sect. B.*, 1981, **37**, 1728.

22 R. D. Adams, I. T. Horváth, and B. E. Segmüller, *Organometallics*, 1982, **1**, 1537.

23 L. J. Farrugia, A. G. Orpen, and F. G. A. Stone, *Polyhedron*, 1983, **2**, 171.

24 D. J. Darensbourg and B. J. Baldwin-Zuschke, *Inorg. Chem.*, 1981, **20**, 3846.

25 V. Albano, P. L. Bellon, and V. Scatturin, *Chem. Commun.*, 1967, 730; F. Demartin, M. Manassero, M. Sansoni, G. Garlaschelli, and U. Sartorelli, *J. Organomet. Chem.*, 1981, **204**, C10; D. F. Chodosh, R. H. Crabtree, H. Felkin, S. Morehouse, and G. E. Morris, *Inorg. Chem.*, 1982, **21**, 1307.

26 H. D. Kaesz, S. A. R. Knox, J. W. Keopke, and R. B. Saillant, *Chem. Commun.*, 1971, 477.

27 R. D. Stephens, *Inorg. Synth.*, 1980, **19**, 87.

28 T. Saito, H. Munakata, and H. Imoto, *Inorg. Synth.*, 1978, **17**, 83.

29 G. Yagupsky and G. Wilkinson, *J. Chem. Soc. A*, 1969, 725.

30 W. Clegg, *Acta Crystallogr., Sect. A*, 1981, **37**, 22.

31 'International Tables for *X*-Ray Crystallography,' Kynoch Press, Birmingham, 1974, vol. 4.

32 SHELX 76, Crystal Structure Solving Package, G. M. Sheldrick, Cambridge, 1976.

Received 29*th December* 1983; *Paper* 3/2281